η^3 and η^6 Bridging Cations in the *N,N,N',N'',N''*-Pentamethyldiethylenetriamine-Solvated Complexes of Benzylpotassium and Benzylrubidium: An X-ray, NMR, and MO Study

Daniele Hoffmann,[†] Walter Bauer,[†] Frank Hampel,[†] Nicolaas J. R. van Eikema Hommes,[†] Paul von Ragué Schleyer,*[,†] Peter Otto,[‡] Ursula Pieper,[§] Dietmar Stalke,[§] Dominic S. Wright,[∥] and Ron Snaith[∥]

Contribution from the Institute of Organic Chemistry and Institute of Theoretical Chemistry, Friedrich-Alexander-Universität Erlangen-Nürnberg, Henkestrasse 42, D-91054 Erlangen, Germany, Institute of Inorganic Chemistry, Georg-August-Universität Göttingen, Tammanstrasse 4, D-37077 Göttingen, Germany, and University Chemical Laboratory, Lensfield Road, Cambridge CB2 1EW, England

Received August 18, 1993[⊗]

Abstract: The metalation of toluene ($PhCH_3$) with a 1:1 mixture of *n*-BuLi/MO^tBu (M = K, Rb) at ambient temperature affords orange-red powders of benzylpotassium or benzylrubidium. On addition of *N,N,N',N'',N''*-pentamethyldiethylenetriamine (PMDTA) the precipitates dissolve to give burgundy-red solutions, from which needles of $[PhCH_2K{\cdot}PMDTA{\cdot}0.5PhCH_3]_n$ (**1**) or $[PhCH_2Rb{\cdot}PMDTA]_n$ (**2**) are obtained. X-ray analysis reveals that **1** incorporates half a molecule of toluene per asymmetric unit. In both **1** and **2**, the η^3 and η^6 interaction of one M^+ cation with two benzyl fragments gives rise to the formation of polymeric chains. The coordination sphere of the cations is completed by one chelating triamine ligand. MO calculations predict multihapto metal carbon interactions to become more important from Li to Cs and substantiate the solid-state results. Ab initio calculations on three different polymers suggest that the array present in the crystal structure is the most stable. The gated decoupled ^{13}C NMR spectrum of **1** in THF-d_8 solution reveals a $^1J(^{13}C,^1H)$ coupling constant for the benzylic carbon atom which may be interpreted in terms of a mainly planar configuration of the CH_2^- group in solution.

Introduction

Unlike organolithium compounds,[1] relatively few structures of synthetically important organic derivatives of the heavier alkali metals have been reported.[2] The more recent investigations of many organosodium[3] as well as several organopotassium[3a,4] structures may be attributed to a growing interest in improved synthetic methods.[5-7] It is now well established that organoalkali reagents $[RM{\cdot}nL]_k$ (R = organic group, M = Li–Cs, L = polar ligands, k = degree of association) are *not* to be regarded as "carbanions".[1c,7] Instead, the alkali metal cation has a pronounced influence on the regio- and stereoselectivity of various reactions.[1c,5b,8] Mixtures of organolithium compounds with potassium (or sodium) alkoxides/amides—termed "super bases" or "complex bases"—are valuable synthetically as they are more reactive than organolithium compounds.[6,7] The exact nature of the metalating species in these mixtures is still unknown. There is evidence that the active species may be a mixed organolithium/alcoholate (amide) aggregate,[9,10] although such a species could not be detected in a NMR study on a model superbase mixture.[11]

Recently, we investigated the influence of alkali metal cations on the solid-state structures of $Ph_3CM{\cdot}nL$ and $C_{13}H_9M{\cdot}nL$ (M

[†] Friedrich-Alexander-Universität Erlangen-Nürnberg, Institute of Organic Chemistry.

[‡] Friedrich-Alexander-Universität Erlangen-Nürnberg, Institute of Theoretical Chemistry.

[§] Georg-August-Universität Göttingen.

[∥] University Chemical Laboratory.

[⊗] Abstract published in *Advance ACS Abstracts*, December 15, 1993.

(1) (a) Setzer, W.; Schleyer, P. v. R. *Adv. Organomet. Chem.* **1985**, *24*, 353. 9b) Wakefield, B. J. *The Chemistry of Organolithium Compounds*; Pergamon Press: Oxford, 1974. (c) Schlosser, M. *Struktur und Reaktivität polarer Organometalle*; Springer-Verlag: Berlin, 1973.

(2) (a) An extensive bibliography is given in the following: Schade, C.; Schleyer, P. v. R. *Adv. Organomet. Chem.* **1987**, *27*, 169. (b) Jutzi, P. *Adv. Organomet. Chem.* **1986**, *26*, 217. (b) Williard, P. G. In *Comprehensive Organic Synthesis*; Trost, B. M., Fleming, I., Eds.; Pergamon Press: Oxford, 1991; Vol. 1, p 1.

(3) (a) Bock, H.; Ruppert, K.; Näther, C.; Havlas, Z.; Herrmann, H.-F.; Arad, C.; Göbel, I.; John, A.; Meuret, J.; Nick, S.; Rauschenbach, A.; Seitz, W.; Vaupel, T.; Solouki, B. *Angew. Chem.* **1992**, *104*, 564; *Angew. Chem., Int. Ed. Engl.* **1992**, *31*, 550 and references therein. (b) Schümann, U.; Behrens, U.; Weiss, E. *Angew. Chem.* **1989**, *101*, 481; *Angew. Chem., Int. Ed. Engl.* **1989**, *28*, 476. (c) Weiss, E.; Corbelin, S.; Cockroft, J. K.; Fitch, A. N. *Angew. Chem.* **1990**, *102*, 728; *Angew. Chem., Int. Ed. Engl.* **1990**, *29*, 650. (d) Schade, C.; Schleyer, P. v. R.; Gregory, P.; Dietrich, H.; Mahdi, W. *J. Organomet. Chem.* **1988**, *341*, 19. (e) Schade, C.; Schleyer, P. v. R.; Dietrich, H.; Mahdi, W. *J. Am. Chem. Soc.* **1986**, *108*, 2482. (f) Gregory, K.; Bremer, M.; Bauer, W.; Schleyer, P. v. R.; Lorenzen, N. P.; Kopf, J.; Weiss, E. *Organometallics* **1990**, *9*, 1485. (g) Corbelin, S.; Lorenzen, N. P.; Kopf, J.; Weiss, E. *Chem. Ber.* **1991**, *124*, 2417. (h) Corbelin, S.; Kopf, J.; Lorenzen, N. P.; Weiss, E. *Angew. Chem.* **1991**, *103*, 875; *Angew. Chem., Int. Ed. Engl.* **1991**, *30*, 825. (i) Gregory, K.; Bremer, M.; Schleyer, P. v. R.; Klusener, P. A. A.; Brandsma, L. *Angew. Chem.* **1989**, *101*, 1261; *Angew. Chem., Int. Ed. Engl.* **1989**, *28*, 1224. (j) Schümann, U.; Weiss, E. *Angew. Chem.* **1988**, *100*, 573; *Angew. Chem., Int. Ed. Engl.* **1988**, *27*, 584. (k) Weiss, E. *Angew. Chem.* **1993**, *105*, 1565; *Angew. Chem., Int. Ed. Engl.* **1993**, *32*, 1501.

(4) (a) Rabe, G.; Roesky, H. W.; Stalke, D.; Pauer, F.; Sheldrick, G. M. *J. Organomet. Chem.* **1991**, *403*, 11. (b) Lorberth, J.; Shin, S.-H.; Wocadlo, S.; Massa, W. *Angew. Chem.* **1989**, *101*, 793; *Angew. Chem., Int. Ed. Engl.* **1989**, *28*, 735. (c) Gregory, K.; Bremer, M.; Schleyer, P. v. R. *Angew. Chem.* **1989**, *101*, 1261; *Angew. Chem., Int. Ed. Engl.* **1989**, *28*, 1224.

(5) (a) Brandsma, L.; Verkruijsse, H. *Preparative Polar Organometallic Chemistry I*; Springer: Berlin, 1987. (b) Brandsma, L. *Preparative Polar Organometallic Chemistry II*; Springer: Berlin, 1990. (c) Pi, R.; Bauer, W.; Brix, B.; Schade, C.; Schleyer, P. v. R. *J. Organomet. Chem.* **1986**, *306*, C1. (d) Schade, C.; Bauer, W.; Schleyer, P. v. R. *J. Organomet. Chem.* **1985**, *295*, C25.

(6) (a) Lochmann, L.; Pospisil, J.; Lim, D. *Tetrahedron Lett.* **1966**, 257. (b) Lochmann, L.; Trekoval, J. *J. Organomet. Chem.* **1987**, *326*, 1. (c) Lochmann, L.; Lim, D. *J. Organomet. Chem.* **1971**, *28*, 153. (d) Lochmann, L.; Petranek, J. *Tetrahedron Lett.* **1991**, *32*, 1483. (e) Lochmann, L. *J. Organomet. Chem.* **1989**, *376*, 1.

(7) (a) Schlosser, M. *J. Organomet. Chem.* **1967**, *8*, 9. (b) Schlosser, M.; Strunk, S. *Tetrahedron Lett.* **1984**, *25*, 741. (c) Schlosser, M.; Hartmann, J. *J. Am. Chem. Soc.* **1976**, *98*, 4674. (d) Stähle, M.; Hartmann, J.; Schlosser, M. *Helv. Chim. Acta* **1977**, *60*, 1730. (e) Schlosser, M.; Lehmann, R. *Tetrahedron Lett.* **1984**, *25*, 745.

(8) Lambert, C.; Schleyer, P. v. R. In *Houben-Weyl: Methoden in der Organischen Chemie*; Hanack, M., Ed.; Thieme Verlag: Stuttgart, 1993; Vol. E 19d, p 1.

0002-7863/94/1516-0528$04.50/0

= K–Cs; L = polar ligands).[12] Compounds of the heavier alkali metals are amenable to X-ray investigations, if stabilized "carbanionic" moieties, i.e π-delocalized systems, are employed. These preclude reactions with the polar ligands. We now present the X-ray structures of $[PhCH_2K\cdot PMDTA\cdot 0.5PhCH_3]_n$ (**1**) and $[PhCH_2Rb\cdot PMDTA]_n$ (**2**), the results of NMR studies of **1** in solution, and supporting semiempirical and ab initio computations on $PhCH_2M$ (M = Li–Cs).

Solid-state structures of $PhCH_2M$ have been reported previously for $[PhCH_2Li\cdot DABCO]_n$,[13] $PhCH_2Li\cdot THF\cdot TMEDA$,[14] $[PhCH_2Li\cdot Et_2O]_n$,[15] $[Li\cdot(TMEDA)_2][Li(TMEDA)Mg(CH_2Ph)_4]$,[16] $[PhCH_2Na\cdot TMEDA]_4$,[3e] $[PhCH_2Na\cdot PMDTA]_n$,[17] as well as for several transition metal complexes.[18] Benzyllithium has been well investigated theoretically[19-22] as well as experimentally.[23] The nature of the Li^+ cation coordination with the benzyl fragment depends on the additional donor ligands present. In the solid-state structures of both benzyllithium and benzylsodium, the cations interact with the center(s) of highest charge. The larger, more polarizable K–Cs cations usually prefer multihapto placements involving more ring carbon atoms.

Results and Discussion

Crystals of **1** and **2** were obtained by treating toluene first with a superbasic 1:1 mixture of *n*-BuLi/KO^{t}Bu[24] and with *n*-BuLi/RbO^{t}Bu, respectively, and then by adding 1.6–2.5 equiv of PMDTA in both cases (eq 1). Such transmetalation reactions

$$PhCH_3 + n\text{-BuLi/MO}^t\text{Bu} \xrightarrow{\text{toluene}} PhCH_2K + BuH + LiO^t\text{Bu} \xrightarrow[\text{1.6–2.5 equiv PMDTA}]{} [PhCH_2M\cdot L]_n \quad (1)$$

M = K, Rb; L = ligand (PMDTA)

are exothermic due to the formation of the strong Li–O bond.[5c,11,25] Crystallizations yielded **1** and **2** exclusively. No mixed aggregate species could be isolated, even if an excess of alcoholate was present.

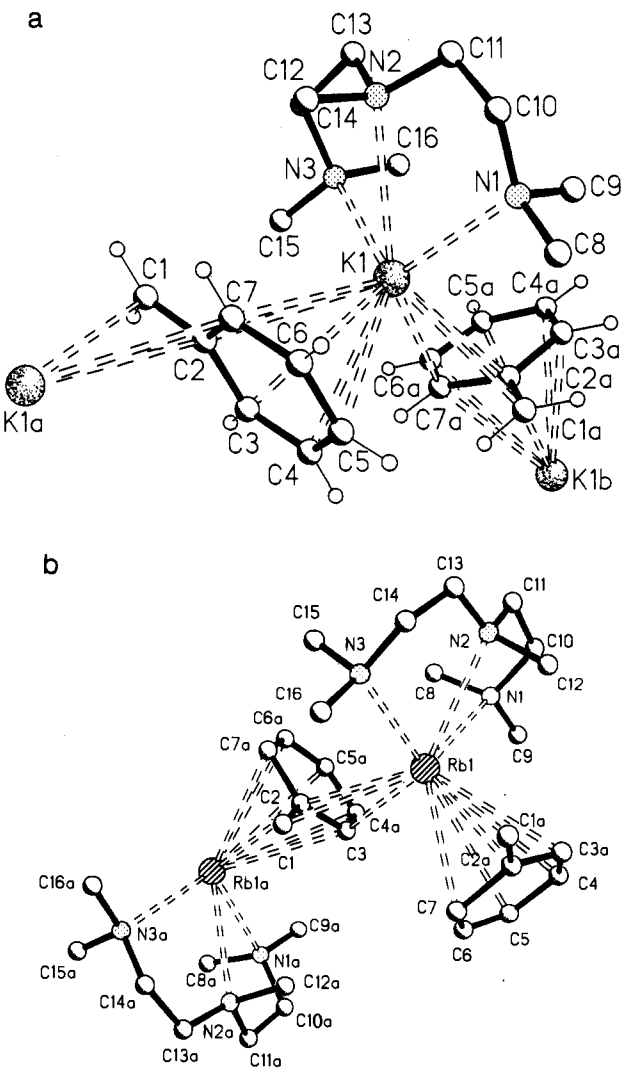

Figure 1. (a) Molecular structure of $[PhCH_2K\cdot PMDTA\cdot 0.5PhCH_3]_n$ (**1**). (b) Molecular structure of $[PhCH_2Rb\cdot PMDTA]_n$ (**2**).

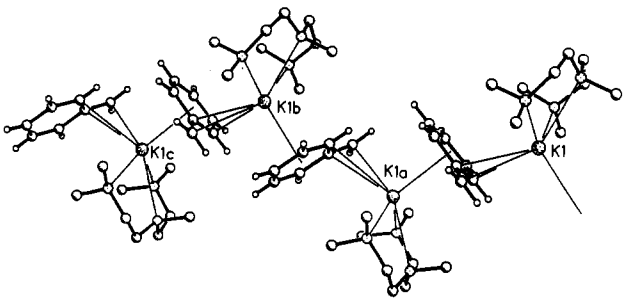

Figure 2. Polymeric zigzag arrangement of $[PhCH_2K\cdot PMDTA\cdot 0.5PhCH_3]_n$ (**1**).

The molecular structures of **1** and **2** (Figure 1a,b) resemble each other. Both compounds display polymeric zigzag arrangements (Figure 2). Tables 1 and 2 give selected geometrical information, and Tables 3 and 4 fractional coordinates and isotropic displacement parameters. As the crystal quality of **2** was poor, most atoms have rather large standard deviations. Hence, we only discuss the "carbanion" geometry of **1** in detail. In both **1** and **2**, each potassium/rubidium ion bridges two benzyl moieties by η^6 and η^3 interactions. The coordination sphere of the cation is completed by a PMDTA ligand (K–N, 284.8(2)–302.8(2) pm; Rb–N, 300.4(23)–311.3(19)).

The two different cation locations in **1** and **2** (η^3 and η^6) are illustrated in Figure 3a,b. The distances involved in the benzylic η^3 coordinations of K^+ and Rb^+ (K–C, 317.1(2)–329.7(2) pm;

(9) (a) Schlosser, M. In *Modern Synthetic Methods*; Scheffold, R., Ed.; VHCA: Basel, Switzerland, 1992; p 227. (b) Mordini, A. In *Advances in Carbanion Chemistry*; Snieckus, V., Ed.; Jai Press Inc.: London, England, 1992; Vol. 1, p 1.
(10) Schlosser, M. *Pure Appl. Chem.* **1988**, *60*, 1627.
(11) Bauer, W.; Lochmann, L. *J. Am. Chem. Soc.* **1992**, *114*, 7482.
(12) (a) Hoffmann, D.; Bauer, W.; Schleyer, P. v. R.; Pieper, U.; Stalke, D. *Organometallics* **1993**, *12*, 1193. (b) Hoffmann, D.; Hampel, F.; Schleyer, P. v. R. *J. Organomet. Chem.* **1993**, *456*, 13.
(13) Patterman, S. P.; Karle, I. L.; Stucky, G. D. *J. Am. Chem. Soc.* **1970**, *92*, 1150.
(14) Zarges, W.; Marsch, M.; Harms, K.; Boche, G. *Chem. Ber.* **1989**, *122*, 2303.
(15) Beno, M. A.; Hope, H.; Olmstead, M. M.; Power, P. P. *Organometallics* **1985**, *4*, 2117.
(16) Schubert, B.; Weiss, E. *Chem. Ber.* **1984**, *117*, 366.
(17) Corbelin, S.; Lorenzen, N. P.; Kopf, J.; Weiss, E. *J. Organomet. Chem.* **1991**, *415*, 293.
(18) See ref 14.
(19) HMO calculations: (a) Brown, D. A.; Dewar, M. J. S. *J. Chem. Soc.* **1953**, 2409. (b) Bingle, W. *Z. Naturforsch.* **1955**, *10a*, 476. (c) Longuet-Higgins, H. C.; Pople, J. A. *Proc. Phys. Soc. (London)* **1955**, *A68*, 591.
(20) Semiempirical studies: (a) Sygula, A.; Rabideau, P. W. *J. Org. Chem.* **1987**, *52*, 3521. (b) Cf. ref 14. (c) Lipkowitz, K. B.; Uhegbu, C.; Naylor, A. M.; Vance, R. *J. Comput. Chem.* **1985**, *6*, 662.
(21) Hard sphere electrostatic (HSE) calculations: (a) Bushby, R. J.; Stell, H. L.; Tytko, P. J. *J. Chem. Soc., Perkin Trans. 2* **1990**, 1155. (b) Bushby, R. J.; Tytko, M. P. *J. Organomet. Chem.* **1984**, *270*, 265.
(22) Ab initio studies: (a) Vanermen, G.; Toppet, S.; Van Beylen, M.; Geerlings, P. *J. Chem. Soc., Perkin Trans. 2* **1986**, 699, 707. (b) Bühl, M.; van Eikema Hommes, N. J. R.; Schleyer, P. v. R.; Fleischer, U.; Kutzelnigg, W. *J. Am. Chem. Soc.* **1991**, *113*, 2459. (c) Sygula, A.; Rabideau, P. W. *J. Am. Chem. Soc.* **1992**, *114*, 821. (d) Anders, E.; Opitz, A.; van Eikema Hommes, N. J. R.; Hampel, F. *J. Org. Chem.* **1993**, *58*, 4424.

Table 1. Selected Bond Lengths (pm) and Angles (deg) of $[PhCH_2K{\cdot}PMDTA{\cdot}0.5PhCH_3]_n$ (1)

K(1)–N(1)	286.9(2)	K(1)–N(2)	302.8(2)
K(1)–N(3)	284.8(2)	K(1)–C(1a)	317.1(2)
K(1)–C(2a)	321.8(2)	K(1)–C(7a)	329.7(2)
K(1)–C(2)	328.8(2)	K(1)–C(3)	322.0(2)
K(1)–C(4)	316.7(2)	K(1)–C(5)	315.0(2)
K(1)–C(6)	319.6(2)	K(1)–C(7)	326.5(2)
C(1)–H(1)	98(2)	C(1)–H(2)	98(2)
C(1)–C(2)	138.1(3)	C(2)–C(3)	144.2(3)
C(2)–C(7)	144.6(3)	C(3)–C(4)	137.0(3)
C(4)–C(5)	139.2(3)	C(5)–C(6)	139.2(3)
C(6)–C(7)	137.9(3)		
N(1)–K(1)–N(2)	59.85(6)	N(2)–K(1)–N(3)	60.91(6)
N(1)–K(1)–N(3)	110.94(7)	H(1)–C(1)–H(2)	121(2)
C(1)–C(2)–C(3)	123.8(2)	C(1)–C(2)–C(7)	123.0(2)
C(3)–C(2)–C(7)	113.2(2)	C(2)–C(3)–C(4)	123.0(2)
C(3)–C(4)–C(5)	122.0(2)	C(4)–C(5)–C(6)	117.2(2)
C(5)–C(6)–C(7)	122.3(2)	C(6)–C(7)–C(2)	122.3(2)

Table 2. Selected Bond Lengths (pm) and Angles (deg) of $[PhCH_2Rb{\cdot}PMDTA]_n$ (2)

Rb(1)–N(1)	306(1)	Rb(1)–N(2)	307(1)
Rb(1)–N(3)	298(1)	Rb(1)–C(1)	327(2)
Rb(1)–C(2)	326(2)	Rb(1)–C(3)	330(2)
Rb(1)–C(2a)	314(2)	Rb(1)–C(3a)	330(2)
Rb(1)–C(4)	349(2)	Rb(1)–C(5)	357(2)
Rb(1)–C(6)	341(2)	Rb(1)–C(7)	326(2)
Rb(1)–C(1a)	373(2)	C(1)–C(2)	139(2)
C(2)–C(3)	145(2)	C(2)–C(7a)	144(2)
C(3)–C(4a)	137(2)	C(4a)–C(5a)	133(2)
C(5a)–C(6a)	134(3)	C(6a)–C(7a)	144(3)
N(1)–Rb(1)–N(2)	57.1(4)	N(2)–Rb(1)–N(3)	58.7(4)
N(1)–Rb(1)–N(3)	107.3(4)	C(1)–C(2)–C(3)	124(2)
C(1)–C(2)–C(7a)	123(2)	C(3)–C(2)–C(7a)	113(2)
C(2)–C(3)–C(4a)	123(2)	C(3)–C(4a)–C(5a)	123(2)
C(4a)–C(5a)–C(6a)	119(2)	C(5a)–C(6a)–C(7a)	123(2)
C(6a)–C(7a)–C(2)	119(2)		

Table 3. Atomic Coordinates ($\times 10^4$) and Isotropic Displacement Parameters ($pm^2 \times 10^{-1}$) of 1

	x	y	z	U(eq)[a]
K(1)	3688(1)	2210(1)	2065(1)	35(1)
C(1)	6343(3)	-633(2)	1899(1)	54(1)
C(2)	5633(2)	-124(2)	2424(1)	42(1)
C(3)	6179(2)	828(2)	2842(1)	46(1)
C(4)	5442(2)	1348(2)	3346(1)	48(1)
C(5)	4098(3)	994(2)	3491(1)	51(1)
C(6)	3542(2)	52(2)	3116(1)	50(1)
C(7)	4260(2)	-499(2)	2609(1)	45(1)
N(1)	732(2)	2472(2)	2050(1)	52(1)
N(2)	1950(2)	1180(2)	914(1)	55(1)
N(3)	4721(2)	2294(2)	730(1)	47(1)
C(8)	195(3)	2434(3)	2732(2)	82(1)
C(9)	742(3)	3701(2)	1808(2)	71(1)
C(10)	-74(3)	1674(3)	1609(2)	77(1)
C(11)	492(3)	1542(3)	916(2)	75(1)
C(12)	2116(4)	-64(3)	1115(2)	79(1)
C(13)	2551(3)	1391(2)	257(1)	69(1)
C(14)	4104(3)	1398(2)	278(1)	68(1)
C(15)	6212(3)	2122(3)	801(2)	75(1)
C(16)	4428(3)	3502(2)	500(1)	60(1)
C(20)	1197(14)	-1451(13)	5614(6)	80(3)
C(21)	482(5)	-520(5)	5185(2)	53(1)
C(22)	1195(14)	102(14)	4704(7)	51(2)
C(23)	544(6)	996(5)	4335(3)	68(2)
C(24)	-823(11)	1249(10)	4438(7)	83(4)
C(25)	-1570(6)	603(7)	4887(5)	84(2)
C(26)	-893(14)	-290(15)	5262(9)	61(4)

[a] U(eq) is defined as one-third of the trace of the orthogonalized U_{ij} tensor.

Rb–C, 326(2)–330(2)) are nearly the same and are governed by contacts to the anion centers of highest charge. The η^6 coordinations correspond to the interaction of K^+/Rb^+ with the

Table 4. Atomic Coordinates ($\times 10^4$) and Isotropic Displacement Parameters ($pm^2 \times 10^{-1}$) of 2

	x	y	z	U(eq)[a]
Rb(1)	1294(1)	-1254(1)	6804(2)	57(1)
C(1)	1777(5)	118(16)	4941(16)	71(5)
C(2)	1410(5)	-358(14)	4163(15)	60(4)
C(3)	978(6)	60(13)	4119(15)	60(4)
C(4)	625(5)	350(15)	8277(15)	59(4)
C(5)	648(6)	1211(17)	7459(20)	84(6)
C(6)	1033(7)	1676(16)	7446(18)	80(6)
C(7)	1422(6)	1335(15)	8315(19)	82(6)
C(8)	645(6)	-3428(16)	4896(17)	82(6)
C(9)	129(5)	-2360(16)	5706(16)	80(6)
N(1)	544(4)	-3045(11)	6014(14)	61(4)
C(10)	523(5)	-4052(15)	6836(20)	80(6)
C(11)	959(6)	-4703(13)	7326(17)	74(5)
N(2)	1306(4)	-3891(11)	7811(16)	75(4)
C(12)	1242(7)	-3398(17)	9004(22)	101(7)
C(13)	1723(6)	-4516(16)	8070(21)	93(7)
C(14)	2100(6)	-3711(17)	8280(22)	95(7)
N(3)	2098(4)	-2749(12)	7385(16)	74(4)
C(15)	2117(7)	-3312(19)	6222(20)	102(7)
C(16)	2471(6)	-1910(21)	7887(21)	102(7)

[a] U(eq) is defined as one-third of the trace of the orthogonalized U_{ij} tensor.

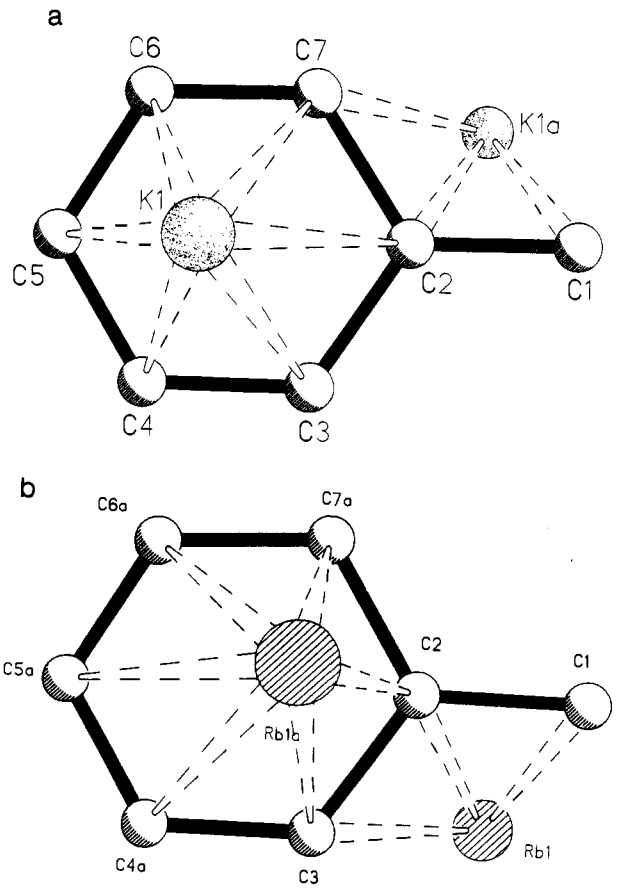

Figure 3. Projection of the molecular structure of **1** (a) and **2** (b), which illustrates the surrounding of the K^+ and Rb^+ cations.

composite negative charge field in the six-membered ring (K–C, 315.0(2)–328.8(2) pm; Rb–C, 314(2)–357(2)). The K^+-η^6 location is almost symmetrical in **1**, with somewhat closer contacts of the cation to the meta and para positions of the ring. In **2**, the Rb^+ location above the phenyl ring is more unsymmetrical; the shortest Rb–C distances are found to the ipso and ortho carbon atoms. Moreover, the Rb(1)–C(1a) distance (373(2) pm) indicates a weak interaction of the cation with the deprotonated methylene carbon atom. Unlike $PhCH_2Li{\cdot}THF{\cdot}TMEDA$,[14] where the CH_2^- group of the benzyl fragment is significantly

pyramidalized, the CH_2^- group in **1** is essentially in the phenylring plane. This allows maximum charge delocalization. The pyramidalization of the CH_2^- group in $PhCH_2Li\cdot THF\cdot TMEDA$ results from the charge-localizing effect of the small Li^+ cation.[2a] A planar benzyl fragment is also present in $[PhCH_2Na\cdot PMDTA]_n$.[17]

The carbon skeleton in **1** exhibits the ring distortion,[26] typically observed in PhX compounds, when X is an electropositive element (e.g. Li–Cs)[3b,27] or an electron-donating group (e.g. CH_2^-).[3a,e,h,12a,15,17] Both σ- and π-delocalization effects are responsible (see Computational Studies). The deviation from regular hexagonal geometry in **1** is characterized by an "elongation" of the ring: rather long C(ipso)–C(ortho) bond lengths of ca. 144 pm, short C(ortho)–C(meta) bond lengths of ca. 137–138 pm, and somewhat longer C(meta)–C(para) distances of ca. 139 pm. To preserve planarity, there is a corresponding change in angles within the ring. The phenyl ring displays an angle contraction at the ipso position (C(3)C(2)C(7) = 113.2(2)°) and a slighter contraction at the para position (117.2(2)°), while the angles at the ortho and meta positions are widened (cf. Table 1).

Whereas **1** prefers a polymeric array, the triphenylmethyl-substituted analog, $Ph_3CK\cdot THF\cdot PMDTA$,[12a] crystallizes as a monomer. Polymerization of the latter may be prevented due to the high steric demand of the propeller-like triphenylmethyl moiety;[12a] a THF molecule completes the coordination sphere of the cation instead. Reducing the steric demand of the anion, i.e. by using $PhCH_2^-$ instead of Ph_3C^-, allows a polymer to form. Even in the presence of a large excess of THF in the reaction mixture, THF does not coordinate to the metal, and **1** is obtained exclusively. Coordination to a second anion moiety is more favorable.

The homologous $[PhCH_2Na\cdot PMDTA\cdot 0.5C_6H_6]_n$[17] also crystallizes in a polymeric zigzag arrangement, but the smaller Na^+ cation bridges the benzyl fragments by η^1 interactions to the C_α-carbons. Hence, there are only two carbon contacts per Na^+ cation. For the larger, more polarizable K^+ and Rb^+ cations, multihapto interactions become more important and nine M–C contacts result overall. As potential energy surfaces of ion pairs involving delocalized carbanions often are quite flat,[28,29] especially with increasing metal to ring distance, different metal cation locations may be observed in the same compound, e.g. in **1** and **2**.[29b] The nature of the haptotropic interaction in **1** and **2** can be expected to change when different polar ligands are present. This has been demonstrated impressively for $Ph_3CK\cdot L_n$ (L = dimethoxyethane, PMDTA, or THF).[30]

η^6 coordinations are found in several potassium compounds: $Ph_3CK\cdot THF\cdot PMDTA$ (K–C, 314–325 pm),[12a] alkali metal graphite intercalates (K–C, 305 pm),[31] $K_2[(Ph_3P)_2(Ph_2PC_6H_4)\text{-}RuH_2]_2\cdot C_{10}H_8\cdot Et_2O$ (K–C, 297–361 pm),[32] $KOsH_3(PMe_2Ph)_3$ (K–C, 312–360 pm),[33] and $K[Nd(O\text{-}2,6\text{-}i\text{-}Pr_2C_6H_3)_4]$ (K–C, 310–347 pm).[34] η^6-K^+-benzene coordinations in lattices are known as well.[35] The reduction of tetraphenylbutadiene with potassium gives a dianion triple salt where K^+ coordinates both η^3 to the chain and η^5 to the ring (K–C, 299–304 and 302–312 pm, respectively). $K(CHPh)_2PPh_2$ exhibits one "classical" benzylic η^3 interaction (K–C,301–325 pm) along with other K–C contacts.[36] An azaallylic η^3 interaction is found in $K\text{-}(2\text{-}C_5H_4N)CHPPh_2CHPPh_2\cdot 2THF$.[37] In $Ph_2(C_5H_4N)CK\cdot PMDTA\cdot THF$, the K^+ cation coordinates to the ipso, ortho, and meta carbon atoms of a phenyl ring (K–C, 314–346 pm) and the nitrogen atom of the pyridyl ring.[38]

Structures of organorubidium compounds are scarce. The Rb–C distances in **2** are in the range observed with other π-delocalized carbanions. These systems include $Rb_2cot\cdot diglyme$ (Rb–C, 310–343 pm),[39] *N*-rubidiocarbazole·PMDTA (Rb–C, 342–368 pm),[40] and $[Ph_3CRb\cdot PMDTA]_n$ (Rb–C, 335–364 pm).[12a] Ab initio calculations on unsolvated bridged allyl rubidium, as expected, predict somewhat shorter Rb–C distances (302.5–305.2 pm).[41]

^{13}C NMR Studies on 1 in THF. $^1J(^{13}C,^1H)$ coupling constants in hydrocarbons are strongly influenced by the hybridization of the carbon atom.[42] The empirically found linear correlation, $^1J(C,H) = 500s[Hz]$, between the magnitude of the coupling constant and the percentage of s-character of the carbon hybrid orbital[43,44] may be used to determine the hybridization at carbon atoms in hydrocarbons qualitatively.[45] Indeed, this correlation also holds for substituted hydrocarbons and even for lithium compounds.[46] $^1J(^{13}C,^1H)$ coupling constants have been employed to evaluate the configuration of benzylic carbon atoms in $PhCH_2M$ compounds.[14,23c,d,g] Assuming that the above correlation may also be applied to benzylic type organolithium compounds, Boche *et al.*[14] concluded that a ca. 125 Hz coupling constant is expected for a tetrahedral (sp^3-hybridized) CH_2^- group, whereas a coupling constant of 167 Hz should result for a planar (sp^2-hybridized) CH_2^- group.[14,42] The small $^1J(^{13}C,^1H)$ coupling constant

(23) (a) Waack, R.; Doran, M. A. *J. Am. Chem. Soc.* **1963**, *85*, 1651. (b) Kuwata, K. *Bull. Chem. Soc. Jpn.* **1960**, *33*, 1091. (c) van Dongen, J. P. C. M.; van Dijkman, H. W. D.; de Bie, M. J. A. *Recl. Trav. Chim. Pays-Bas* **1974**, *93*, 29. (d) Takahashi, K.; Koudo, Y.; Asami, R. *Org. Magn. Reson.* **1974**, *6*, 580. (e) Sandel, V. R.; Freedman, H. H. *J. Am. Chem. Soc.* **1967**, *89*, 4395. (f) Asami, R.; Levy, M.; Szwarc, M. *J. Chem. Soc.* **1962**, 361. (g) Waack, R.; Doran, M. A.; Baker, E. B.; Olah, G. A. *J. Am. Chem. Soc.* **1966**, *88*, 1272. (h) Waack, R.; McKeever, D. L.; Doran, M. A. *Chem. Commun.* **1969**, 117.

(24) Schlosser, M.; Hartmann, J. *Angew. Chem.* **1973**, *85*, 544; *Angew. Chem., Int. Ed. Engl.* **1973**, *12*, 508.

(25) van Eikema Hommes, N. J. R.; Schleyer, P. v. R. Unpublished results.

(26) (a) Dunitz, J. D.; Wallis, J. D. *Helv. Chim. Acta* **1984**, *67*, 1374. (b) Domenicano, A.; Murray-Rust, P.; Vaciago, A. *Acta Crystallogr.* **1983**, *B39*, 457 and references therein. (c) Domenicano, A.; Vacagio, A.; Coulson, C. A. *Acta Crystallogr.* **1975**, *B31*, 1630. (d) Domenicano, A. In *Accurate Molecular Structures*; Domenicano, A., Hargittai, J., Eds.; Oxford University Press: New York, 1992; p 437.

(27) (a) Maetzke, T.; Seebach, D. *Helv. Chim. Acta* **1989**, *72*, 624. (b) Hope, H.; Power, P. P. *J. Am. Chem. Soc.* **1983**, *105*, 5320. (c) Thoennes, D.; Weiss, E. *Chem. Ber.* **1978**, *111*, 3157. (d) Stalke, D.; Whitmire, K. *J. Chem. Soc., Chem. Commun.* **1990**, 833. (e) Harder, S.; Ekhart, P. F.; Brandsma, L.; Kanters, J. A.; Duisenberg, A. J. M.; Schleyer, P. v. R. *Organometallics* **1992**, *11*, 2623.

(28) (a) Schleyer, P. v. R. *Pure Appl. Chem.* **1983**, *55*, 355. (b) Schleyer, P. v. R. *Pure Appl. Chem.* **1984**, *56*, 151.

(29) (a) Streitwieser, A. *Acc. Chem. Res.* **1984**, *17*, 353. (b) Boche, G.; Etzrod, H.; Massa, W.; Baum, G. *Angew. Chem.* **1985**, *97*, 858; *Angew. Chem., Int. Ed. Engl.* **1985**, *24*, 863.

(30) Viebrock, H. Ph.D. dissertation, Hamburg, 1992.

(31) (a) Rüdorff, W. *Adv. Inorg. Radiochem.* **1959**, *1*, 223. (b) Solin, S. A. *Adv. Chem. Phys.* **1982**, *49*, 455. (c) Levy, F. *Intercalated Layered Materials*; Reidel: Dordrecht, 1979.

(32) Pez, G. P.; Grey, R. A.; Corsi, J. *J. Am. Chem. Soc.* **1981**, *103*, 7528.

(33) Huffman, J. C.; Green, M. A.; Kaiser, S. L.; Caulton, K. G. *J. Am. Chem. Soc.* **1985**, *107*, 5111.

(34) Clark, D. L.; Watkin, J. G.; Huffman, J. C. *Inorg. Chem.* **1992**, *31*, 1556.

(35) (a) Atwood, J. L.; Hrncir, D. C.; Priester, R. D.; Rogers, R. D. *Organometallics* **1983**, *2*, 985. (b) Atwood, J. L.; Hrncir, D. C.; Rogers, R. D. *J. Inclusion Phenom.* **1983**, *1*, 199. (c) Atwood, J. L.; Crissinger, K. D.; Rogers, R. D. *J. Organomet. Chem.* **1978**, *155*, 1. (d) Atwood, J. L. *J. Inclusion Phenom.* **1985**, *3*, 113. (e) Atwood, J. L. *Recent Dev. Sep. Sci.* **1977**, *3*, 195.

(36) Schmidbaur, H.; Deschler, U.; Milewski-Mahrla, B.; Zimmer-Gasser, B. *Chem. Ber.* **1981**, *114*, 608.

(37) Schmidbaur, H.; Deschler, U.; Milewski-Mahrla, B. *Chem. Ber.* **1982**, *115*, 3290.

(38) Pieper, U.; Stalke, D. *Organometallics* **1993**, *12*, 1201.

(39) Noordik, J. H.; Degens, H. M. L.; Mooji, J. J. *Acta Crystallogr.* **1975**, *B31*, 2144.

(40) Gregory, K. Ph.D. Thesis, Universität Erlangen-Nürnberg, 1991.

(41) Hommes, N. J. R.; Schleyer, P. v. R. *J. Organomet. Chem.* **1991**, *409*, 307.

(42) Kalinowski, H.-O.; Berger, S.; Braun, S. *^{13}C-NMR-Spektroskopie*; Georg Thieme Verlag: Stuttgart, 1984; p 445.

(43) Muller, N.; Pritchard, D. E. *J. Chem. Phys.* **1959**, *31*, 768.

(44) (a) Newton, M. D.; Schulman, J. M.; Manus, M. M. *J. Am. Chem. Soc.* **1974**, *96*, 17. (b) Lett, R.; Chassaing, G.; Marquet, A. *J. Organomet. Chem.* **1976**, *111*, C17.

(45) (a) Mislow, K. *Einführung in die Stereochemie*; VCH Verlagsgesellschaft: Weinheim, 1972. (b) Bingel, W. A.; Lüttke, W. *Angew. Chem.* **1981**, *93*, 944; *Angew. Chem., Int. Ed. Engl.* **1981**, *20*, 899.

(46) Schleyer, P. v. R.; van Eikema Hommes, N. J. R. Unpublished results.

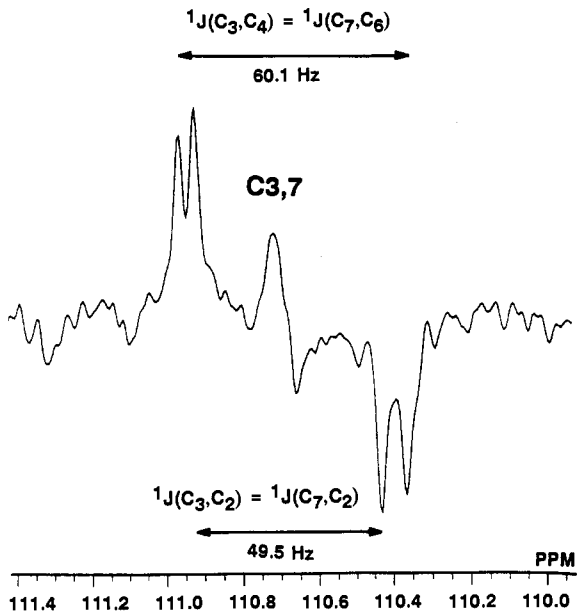

Figure 4. INADEQUATE spectrum of **1** in THF-d_8, $T = -10$ °C; spectral width, 7575.8 Hz; number of data points, 32 768; relaxation delay, 8.0 s; C3,7 region expanded.

observed for CH_3Li (98 Hz)[47] results from a rehybridization of the carbon atom, which is no longer sp^3 hybridized.[46] For $PhCH_2Li$[23c,d] and $PhCH_2Li$·THF·TMEDA[14] in THF-d_8, $^1J(^{13}C,^1H)$ values of 134 and 131 Hz, respectively, were determined for the benzylic carbon atoms. These values were interpreted in terms of a pyramidalized CH_2^- group.[14] In the gated decoupled ^{13}C NMR spectrum of **1** (THF-d_8, −20 °C), we observed a significantly larger coupling constant of 151.1 Hz, which would approximately correspond to an $sp^{2.3}$ hybridization and is in accord with a nearly planar configuration of the CH_2^- group. Hence, the planarization of the benzylic carbon atom in the solid-state structures of $PhCH_2M$ with M = Li–K is reflected in solution by an increase of the $^1J(^{13}C,^1H)$ value.

The ring distortion observed in the solid-state structure of **1** (and of PhX derivatives in general) has been attributed to hybridization changes at the substituted carbon atom.[26] According to Walsh[48a] and Bent,[48b] an electropositive (i.e. X = Li–Cs) or electron-donating substituent (i.e. X = CH_2^-) should increase the p-character in the C(ipso)–C(ortho) bonds, thus resulting in an elongation of these bonds and an angle contraction at the ipso position, as observed in **1**. Since $^1J(^{13}C,^{13}C)$ is very sensitive to the hybridization at both carbon atoms, such coupling constants can provide additional experimental information concerning the observed ring distortion.[42] This has been demonstrated recently for phenyllithium,[27e] where the very small C(ipso)–C(ortho) coupling constant of 27.8 Hz was interpreted in terms of a considerable decrease in s-character in the carbon-bonding hybrids as compared to benzene (56.0 Hz). To evaluate the influence of the CH_2^- substituent on the $^1J(^{13}C,^{13}C)$ coupling constant, we recorded the INADEQUATE[49] ^{13}C spectrum of **1** in THF-d_8 at +2 °C (Figure 4). The observed $^1J(^{13}C,^{13}C)$ C(ipso)–C(ortho) coupling constant of 49.5 Hz is smaller than in benzene, but significantly larger than in phenyllithium (27.8 Hz). Thus, one might speculate that the ring deformation in **1** is less pronounced than in phenyllithium.[27e] However, as coupling constants in unsaturated C–C bonds are influenced by additional orbital dipole (J^{OD}) and spin-dipolar (J^{SD}) noncontact coupling terms, the amount of s-character in the relevant bond cannot be determined quantitatively.[44a] Therefore, a direct comparison of the ring distortion in **1** and in phenyllithium based on the C(ipso)–C(ortho) coupling constants is precluded (for a more detailed discussion; cf. Computational Studies).

The same coupling constant as in **1** was observed in $PhSiH_3$.[50] With electronegative substituents such as Cl or F the $^1J(^{13}C,^{13}C)$ coupling constants are larger (65.2 and 70.8 Hz, respectively), as expected.[50]

Computational Studies. 1. Ab Initio Investigation of PhX Species. The trend toward polyhapto bonding between the metal cation and the benzyl anion on going from lithium to cesium is substantiated by the computed $PhCH_2M$ structures (Figure 5). The small lithium cation can coordinate in several ways. In the most stable form, **3**, lithium "binds" η^3 to the benzylic and one ortho carbon atom. Alternatively, lithium can interact with the ring in a η^5 fashion (**4**). While **4** is less stable than **3** by 2.2 kcal/mol, it is a minimum and has a barrier of 0.9 kcal/mol toward rearrangement into the η^3 haptomer **3**. A η^2 structure, **5**, with Li^+ in the plane of symmetry, represents the transition structure (with an activation barrier of 0.1 kcal/mol) between the two possible enantiomeric η^3 minima, **3**. The contact to the ortho carbon atoms in **5** is weaker than in **3**.

Table 5 lists the natural charges[51] on the metal cations and on the CH groupings (hydrogen charges were added to the charge on the carbon atom). Note the effect of the lithium cation on the charge distribution in the "anion": both in **3** and **4**, the negative charge in the benzyl moiety is significantly more localized (by the lithium cation) than in the free benzyl anion.

For benzylsodium, **6**, only one minimum, in which Na^+ binds η^4 to the benzyl anion, could be located. Both η^3 and η^5 starting geometries reverted to **6** upon optimization. The longer C–Na bonds allow effective contacts to C_α and to both ortho carbon atoms, which represent the centers of highest negative charge.

The heavier alkali metals, K, Rb, and Cs, are large enough to contact all carbon atoms. Structures **7–9**, in which the metal binds η^7 to the benzyl anion, result. The charges in the benzyl fragment are much more delocalized than with lithium or sodium and approach the free benzyl anion situation. The charges on the metal increase to almost unity.

Structure optimization at a correlated level, with inclusion of the metal-centered core ($n - 1$) electrons, is essential (we used MP2(full) in the present work). As demonstrated previously for the alkali metal hydrides,[52] SCF-computed metal hydride distances are much too long for M = K, Rb, and Cs, while MP2-optimized M–H distances deviate only slightly from the experimental values. The same situation pertains to the $M–CH_3$ and M–Cp structures.[52] This shortening of the metal ligand bond at correlated levels is due to core–valence correlation.[53] At the SCF level, the repulsion between the metal core ($n - 1$) electrons and the anion valence electrons is overestimated. Hence, metal–benzyl distances, optimized at SCF level, are significantly longer than the MP2-optimized values. For benzylpotassium, a η^2 rather than a η^7 structure is obtained at SCF.

While the isolated benzyl anion is planar, the Coulombic interaction with the metal cation results in deformation from planarity. The ring is folded, and C_α is pyramidalized to some extent. Nevertheless, the main structural features in the carbanion moieties remain (Table 6). The ipso angles are strongly contracted. To a lesser extent, the same is true for the para angles, while the ortho and meta angles are widened. In addition,

(47) McKeever, L. D.; Waack, R.; Doran, M. A.; Baker, E. B. *J. Am. Chem. Soc.* **1969**, *91*, 1057.
(48) (a) Walsh, A. D. *Discuss. Faraday Soc.* **1947**, *2*, 18. (b) Bent, H. A. *Chem. Rev.* **1961**, *61*, 275.
(49) Bax, A.; Freeman, R.; Kempsell, S. P. *J. Am. Chem. Soc.* **1980**, *102*, 4851.
(50) Wray, V.; Ernst, L.; Lund, T.; Jakobsen, H. J. *J. Magn. Reson.* **1980**, *40*, 55.
(51) (a) Reed, A. E.; Weinstock, R. B.; Weinhold, F. *J. Chem. Phys.* **1985**, *83*, 735. (b) Reed, A. E.; Curtis, L. A.; Weinhold, F. *Chem. Rev.* **1988**, *88*, 889.
(52) Lambert, C.; Kaupp, M.; Schleyer, P. v. R. *Organometallics* **1993**, *12*, 853.
(53) Fuentealba, P.; Reyers, O.; Stoll, H.; Preuss, H. *J. Chem. Phys.* **1987**, *87*, 5338.

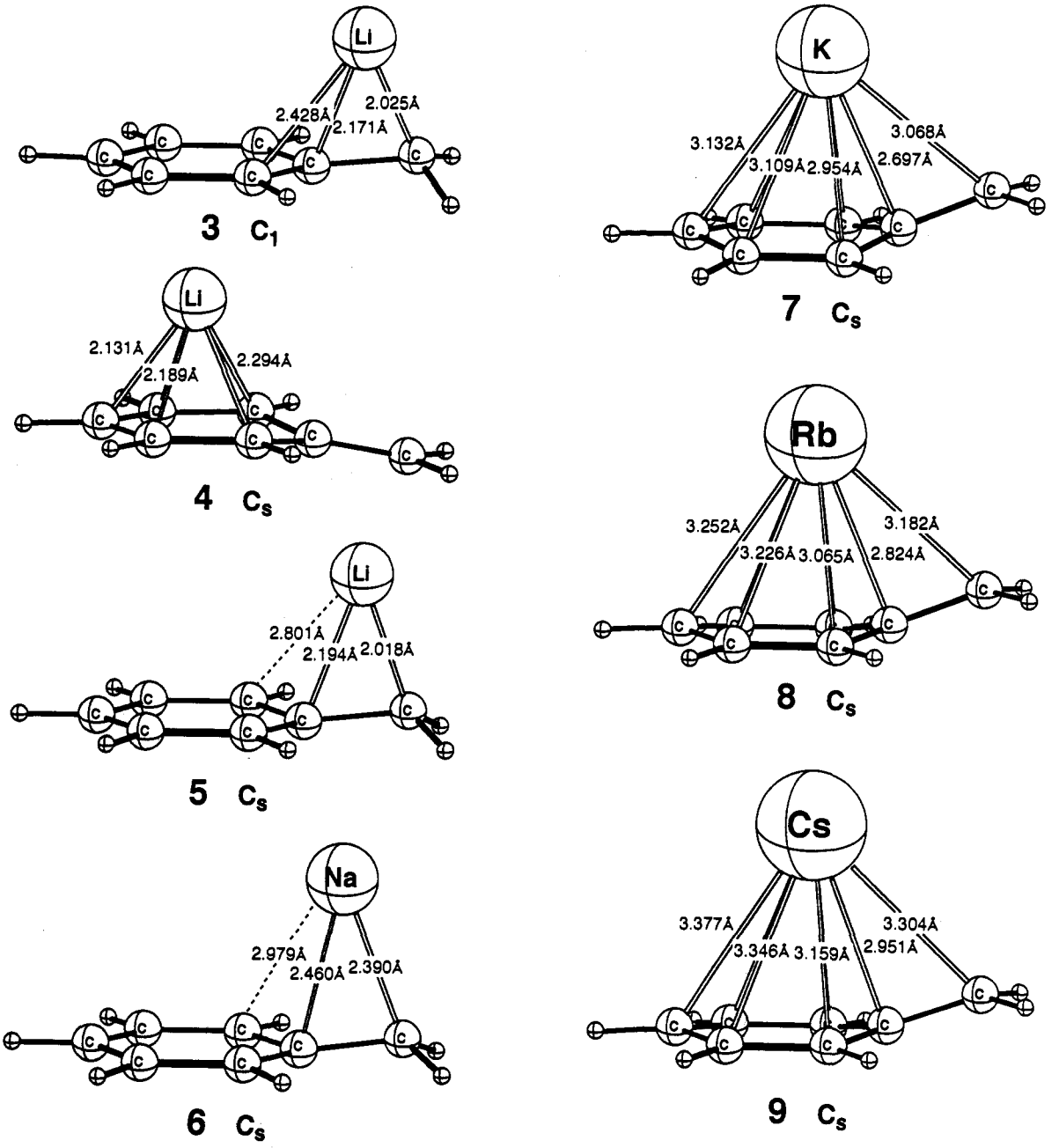

Figure 5. MP2-optimized geometries of $PhCH_2M$ (M = Li–Cs).

Table 5. NPA Charges, Calculated from the Correlated Density Matrix, with Hydrogen Charges Added to the Carbon Charge

		C_{ipso}	$C_\alpha + 2H$	$C_{ortho} + H$	$C_{meta} + H$	$C_{para} + H$	M
$PhCH_2Li$	η^3	−0.083	−0.552	−0.195[a]	0.041[a]	−0.081	0.891
				−0.057	0.035		
	η^5	−0.088	−0.158	−0.164	−0.025	−0.284	0.908
$PhCH_2Na$	η^2	−0.069	−0.525	−0.111	0.020	−0.100	0.874
$PhCH_2K$	η^7	−0.077	−0.359	−0.128	−0.011	−0.207	0.922
$PhCH_2Rb$	η^7	−0.040	−0.398	−0.151	0.014	−0.229	0.942
$PhCH_2Cs$	η^7	−0.045	−0.397	−0.160	0.019	−0.233	0.956
$PhCH_2^-$		+0.010	−0.445	−0.162	0.013	−0.269	

[a] Ortho and meta carbon atoms closest to Li.

the C(ipso)–C(ortho) bonds are strongly elongated. The calculated angles agree very well with the X-ray values.

With the exception of the contraction of the para angles, these distortions are typical for benzene rings with an electropositive, σ-donating substituent.[26d] Electronegative substituents cause the opposite geometrical deformations: the ipso angle is widened, the ortho angle contracted, and the C(ipso)–C(ortho) bond shortened. The para angle shows very little variation with the electronegativity of the substituent.

Substituents with lone pairs or empty p-orbitals may lead to additional structural distortions. Both π-donating and π-accepting substituents cause a contraction of the ipso angle. In addition, a π-donating substituent causes the para angle to decrease, while a widening occurs with a π-acceptor. These combined π-effects are easily demonstrated in the free benzyl cation and anion, in which π-effects can be "shut off" by a 90° rotation of the CH_2 group. In $PhCH_2^+$, the rotation of CH_2^+ leads to a widening of the ipso angle by almost 2° and a decrease in the para angle by the same amount (Table 6). In $PhCH_2^-$, the rotation of the CH_2^- group results in the widening of the ipso angle by 1° and of the para angle by about 2°. Corresponding changes are seen in the ortho and meta angles.

On the basis of these ring deformations, the CH_2^- substituent can be considered as a strongly electropositive substituent with both σ- and π-donor capabilities. The same holds for the CH_2M substituent. The ring distortions due to σ-effects in benzylpotassium, -rubidium, and -cesium are comparable to that in

Table 6. Calculated Bond Lengths and Bond Angles of Benzyl Alkali Metals and Reference Species

		∠ipso	∠ortho	∠meta	∠para	C_i–C_o	C_o–C_m	C_m–C_p	C_i–C_α
$PhCH_2Li$	η^3	114.8	122.5[a]	121.2[a]	118.4	1.425[a]	1.388[a]	1.390[a]	1.443
			122.3	120.6		1.429	1.400	1.402	
$PhCH_2Na$	η^2	114.9	122.5	121.0	118.2	1.424	1.393	1.398	1.447
$PhCH_2K$	η^7	113.4	121.7	121.4	116.9	1.422	1.389	1.411	1.399
$PhCH_2Rb$	η^7	113.4	122.0	121.5	116.8	1.442	1.388	1.411	1.398
$PhCH_2Cs$	η^7	113.4	122.4	121.6	116.6	1.443	1.388	1.410	1.395
$PhCH_2^-$		113.5	123.0	121.9	116.8	1.442	1.389	1.408	1.396
	perp	114.5	123.2	120.3	118.7	1.420	1.401	1.398	1.475
$PhCH_2^+$		120.3	119.3	119.4	122.3	1.436	1.378	1.408	1.372
	perp	122.1	117.8	121.1	120.1	1.412	1.393	1.394	1.421
PhLi		114.3	123.4	119.8	119.2	1.414	1.398	1.394	
$PhCH_3$		118.4	122.0	120.1	119.5	1.399	1.394	1.395	
PhF		122.5	118.4	120.4	119.9	1.388	1.395	1.396	

[a] Ortho and meta carbon atoms closest to Li.

Table 7. Calculated Ipso Angle, C_{ipso}–C_{ortho} Bond Lengths, NLMO % s-Contributions, and Calculated and Experimental ^1J(C–C) Coupling Constants for PhX Species

X	∠ipso[a]	C_{ipso}–C_{ortho}[a]	% s (C_{ipso})[a]	% s (C_{ortho})[a]	J_{calc}[b]	J_{exp}
F	122.5	1.388	35.9	29.7	72.6	70.8[c]
OH	120.3	1.396	33.7	30.0	65.8[c]	67.0[c]
NH_2	118.8	1.401	31.4	30.8	60.4[c]	61.2[c]
CH_3	118.4	1.399	29.8	31.4	56.2[c]	57.0[c]
BH_2	117.8	1.404	27.9	31.6	49.4[c]	48.4[c]
BeH	116.7	1.411	32.4	31.9	68.7	
Li	114.3	1.414	34.7	33.1	83.0	27.8
CH_2^-	113.5	1.442	27.2	31.3	45.8	(49.5)
CH_2K	113.4	1.442	26.7	30.6	41.4	49.5

[a] Calculated at MP2(full)/6-31G* level, MP2(full)/6-31+G* for X = CH_2^-. [b] Coupling constants calculated from the correlation of the product of % s (C_{ipso}) and % s (C_{ortho}) with the experimental values. [c] Coupling values used in the correlation.

phenyllithium. On the other hand, the $^1J(^{13}C_{ipso},^{13}C_{ortho})$ coupling constants differ significantly: 49.5 Hz for **1** and 27.8 Hz for phenyllithium.

Can experimental C–C coupling constants be used to estimate the amount of s-character in the C–C bonds in these systems? The relationship between hybridization and coupling constant is based on the assumption that the coupling is mainly determined by the Fermi contact term, which is proportional to the product of the % s-character in the hybrids comprising the C–C bond.[42] However, in unsaturated C–C bonds, additional orbital dipole (J^{OD}) and spin-dipolar (J^{SD}) noncontact coupling terms may become important.[44a]

The s-contributions to the C_{ipso}–C_{ortho} bonds of several PhX derivatives, which were calculated from the NLMO hybridizations, are presented in Table 7. For X = F, OH, NH_2, CH_3, and BH_2, the hybridization, as well as the ipso angle and C_{ipso}–C_{ortho} bond length, shows the variation with substituent electronegativity following Walsh's rule.[48] For these substituents, the product of % s (C_{ipso}) and % s (C_{ortho}) correlates reasonably well with the experimental coupling constants. This suggests that in these cases, the Fermi contact term is the main contribution to C–C coupling. Interestingly, even the C_{ipso}–C_{ortho} coupling constant obtained from this correlation for the free benzyl anion (45.8 Hz) is in acceptable agreement with the experimental value of 49.5 Hz observed for **1**. The calculated coupling constant of $PhCH_2K$ (41.4 Hz) deviates more, as the $PhCH_2^-\cdots K^+$ interactions in the isolated molecule, where the unsolvated potassium is coordinatively unsaturated, are exaggerated.

The bonding situation is different in PhLi and PhBeH. The hybridizations calculated for C_{ipso} and C_{ortho} do not follow the trend. Despite the small ipso angles and long C_{ipso}–C_{ortho} bonds, the hybrids contain more s-character than for, for example, X = BH_2. Thus, the above correlation would give a C–C coupling of 83 Hz. This outcome supports the conclusion by Harder *et al.*[27e] that other terms besides the Fermi contact term likely contribute to the C–C coupling in phenyllithium.

Table 8. Heats of Formation ΔH_f and Solvation Enthalpies ΔH_{solv} (in kcal/mol) for 1 (ΔH_f for PMDTA and THF, 15.6 and −59.3 kcal/mol)[52]

	$PhCH_2K$	$PhCH_2K$·PMDTA	$PhCH_2K$·PMDTA·THF
ΔH_f	−62.9	−147.2	−201.6
ΔH_{solv}		−99.9	−95.0
hapticity	η^6	η^6	η^6

The energetic preference for the geometry present in the X-ray structure of **1** is supported by preliminary single-point ab initio calculations (2_1 screw axis symmetry restriction, first neighbors' approximation; cf. Experimental Section) on three different polymeric chains. The possible alternatives considered were (1) the polymeric chain present in the X-ray structure of **1** with unsymmetrical η^3 and η^6 bridging K^+ cations; (2) a hypothetical polymer with symmetrically η^6/η^6 bridging K^+ cations, i.e. coordination of K^+ to the phenyl rings; and (3) a hypothetical polymer in which the K^+ gegenions symmetrically bridge the benzyl fragments by a η^3/η^3 interaction with the allylic positions. The hypothetical polymers were "constructed" by applying symmetry operations to the fragments of the X-ray structure, in which K^+ is η^6 or η^3 coordinated. The η^3/η^6 bridged polymer (X-ray geometry) is 61 kcal/mol (per monomeric unit) more stable than the η^6/η^6 bridged form and 94 kcal/mol (per monomeric unit) more stable than the η^3/η^3 bridged form. Even when allowing for significant errors due to the use of nonoptimum geometries in the calculations of the hypothetical polymers, the overall energetic order is not expected to change.[54] The preference for unsymmetrical bridging presumably results from the more effective delocalization of the negative charge (i.e. over the whole benzyl fragment) than in the symmetrically bridged polymers.

2. MNDO Investigations. General structural features of organolithium compounds have often been predicted by semiempirical MNDO calculations.[55a] We used this method as implemented in the VAMP program[55b] to test MNDO potassium parameters, which were developed recently.[56] $PhCH_2K$, $PhCH_2K$·PMDTA, and $PhCH_2K$·PMDTA·THF were optimized without symmetry constraints using several different starting geometries. Heats of formation, solvation energies, and hapticities are given in Table 8. The MNDO ΔH_f values for PMDTA and THF were taken from the literature.[57] In all three species calculated, potassium is η^6-bound; no local η^3 minimum could be found. The geometry of the benzyl fragment in $PhCH_2K$ deviates significantly from planarity, with a folded phenyl ring. Qualitatively, the deformation of the phenyl ring agrees with that in

(54) Lambert, C.; Schleyer, P. v. R.; Newton, M. G.; Schreiner, P. *Z. Naturforsch.* **1992**, *B47*, 869.

(55) (a) Dewar, M. J. S.; Thiel, W. *J. Am. Chem. Soc.* **1977**, *99*, 4899, 4907. (b) VAMP (vectorized ampac): Rauhut, G., Chandrasekar, J., Clark, T., Erlangen, 1991.

(56) Havlas, Z., Institute of Organic Chemistry and Biochemistry, Czechoslovak Academy of Sciences, Prague, unpublished.

(57) Kaufmann, E.; Gose, J.; Schleyer, P. v. R. *Organometallics* **1989**, *8*, 2577.

the ab initio calculated structure. Solvation of K^+ by PMDTA ($PhCH_2K$·PMDTA) is exothermic by –99.9 kcal/mol. Additional solvation by a THF ligand (several different starting geometries were used) usually led to extrusion of this second ligand, implying that the K^+ cation was "oversolvated" by the additional THF. One $PhCH_2K$·PMDTA·THF minimum with both THF and PMDTA coordinated could be localized, but this species is 4.9 kcal/mol less stable than $PhCH_2K$·PMDTA. Moreover, in this structure one terminal nitrogen of the PMDTA and the oxygen of the THF ligand are only weakly coordinated to the K^+ cation (rather long K–N and K–O distances). The MNDO results agree with the fact that THF—even if present in large excess—does not coordinate to **1**. However, we have previously shown[12a] that THF coordination is also found by MNDO to be unfavorable for Ph_3CK·PMDTA·THF, although in this case THF does coordinate to the K^+ cation in the crystal. MNDO fails to reproduce the experimentally observed η^3 minimum of **1**, as it overestimates K–C interaction energies. The provision K-parametrization[56] underestimates K–C distances (ca. 50 pm too short) to a greater extent than K–N distances (ca. 10 pm too short).

Conclusions

Multihapto interactions with the benzyl fragment become more important along the alkali metal series M = Li to M = Rb. Both the polar ligands (i.e. PMDTA, THF) and the carbanion moiety compete for the alkali metal cation. For small cations (Li^+ and Na^+), the interaction with strong polar ligands is more favorable energetically. For the larger, more polarizable K^+ and Rb^+ cations, the interaction with a second carbanion is preferred. The similarity of the structures of **1** and **2** suggests the coordination requirement of the heavier alkali metals (K–Cs) to be similar. That polymers form rather than finite aggregates may be rationalized by simple electrostatic models: the attractive Coulombic energy for an infinite chain of alternating unit charges is higher than for a finite cluster.[54]

Experimental Section

All manipulations were carried out under an argon atmosphere by using standard Schlenk and needle/septum techniques. All solvents were freshly distilled from Na/K alloy under argon. PMDTA was dried over CaH_2 for several days, distilled, and subsequently kept over Na/Pb alloy under argon. KO^{t}Bu was used without further purification as purchased from Aldrich. RbO^{t}Bu was prepared by reacting Rb metal with ^{t}BuOH in THF for 1 week. After removing THF in vacuo, a white powder is obtained, which can be stored indefinitely under argon.

$[PhCH_2K$·PMDTA·0.5$PhCH_3]_\infty$ 1. At ca. 0 °C, 5.5 mL of *n*-BuLi (1.6 M in hexane; 8.8 mmol) was added dropwise to a well-stirred suspension of KO^{t}Bu (1.0 g, 8.9 mmol) in 30 mL of toluene.[24] This caused an orange-red solid to precipitate, which dissolved on addition of 4.7 mL (22.0 mmol) of PMDTA upon gentle heating. Cooling the solution to room temperature instantaneously afforded microcrystalline needles. Crystals of X-ray quality were obtained from the filtrate after storing it at +4 °C for 3 days. Total yield: 2.085 g (67%). Anal. Calcd for $C_{19.5}H_{34}N_3K$: C, 66.99; H, 9.80; N, 12.02. Found: C, 66.67; H, 9.82; N, 12.18. ^{1}H NMR (400 MHz, THF-d_8, 0 °C), in ppm: δ 6.05 (2H, dd, J = 6.7, 8.2 Hz, *m*-H), 5.54 (2H, d, J = 8.2 Hz, *o*-H), 4.72 (1H, t, J = 6.7 Hz, *p*-H), 2.21 (2H, s, $PhCH_2$); PMDTA signals at δ 2.41 and 2.31 (4H, t, J = 7.0 Hz, NCH_2) 2.19 (3H, s, NCH_3), 2.15 (12H, s, NCH_3); toluene signals at δ 7.13 (2.5H, m, C_6H_5), 2.31 (1.5 H, s, $PhCH_3$), the latter signal overlaps with one NCH_2 signal of PMDTA. Integration may indicate variable amounts of toluene, as this is easily lost when the product is dried in vacuo. ^{13}C NMR (100 MHz, THF-d_8, 0 °C), in ppm: δ 152.99 (*ipso*-C), 130.25 (*m*-C), 110.90 (*o*-C), 95.15 (*p*-C), 52.58 (C(1)); PMDTA signals at δ 58.58 and 57.17 (CH_2), 45.98 (CH_3, terminal), 42.87 (CH_3, central); toluene signals at δ 138.27 (*ipso*-C), 129.62 (*o*-C), 128.90 (*m*-C), 126.03 (*p*-C), 21.51 (C(1)).

It should be noted that large crystals of **1** may even be obtained in the presence of a 20-fold excess of THF at room temperature. However, if these crystals are isolated and redissolved in THF-d_8, the solution is no longer stable above 0 °C.

$[PhCH_2Rb$·PMDTA$]_\infty$ 2. The reaction was carried out as described for **1**, using 20 mL of toluene, 1.02 g (6.44 mmol) of RbO^{t}Bu and 4.0 mL (6.44 mmol) of *n*-BuLi (1.6 M in hexane). The resulting orange-red precipitate was dissolved by adding 2.2 mL (10.28 mmol) of PMDTA at ambient temperature. After 1 h microcrystalline needles had formed. Crystals of X-ray quality were obtained from the filtrate after storing it at +4 °C for 1 week. Total yield: 1.31 g (58%). Anal. Calcd for $C_{16}H_{30}N_3Rb$: C, 54.92; H, 8.64; N, 12.01. Found: C, 54.82; H, 8.67; N, 12.05. ^{1}H NMR (400 MHz, THF-d_8, 0 °C), in ppm: δ 6.02 (2H, dd, J = 6.7, 8.5 Hz, *m*-H), 5.46 (2H, d, J = 8.5 Hz, *o*-H), 4.69 (1H, t, J = 6.7 Hz, *p*-H), 2.25 (2H, s, $PhCH_2$); PMDTA signals at δ 2.39 and 2.29 (4H, t, J = 6.3 Hz, NCH_2), 2.19 (3H, s, NCH_3), 2.15 (12H, s, NCH_3). ^{13}C NMR (100 MHz, THF-d_8, 0 °C), in ppm: δ 152.55 (*ipso*-C), 130.53 (*m*-C), 111.08 (*o*-C), 94.74 (*p*-C), 54.57 (C(1)); PMDTA signals at δ 58.32 and 57.06 (CH_2), 45.83 (CH_3, terminal), 42.37 (CH_3, central).

X-ray Measurement. Crystal data for 1: M_r = 349.60, monoclinic, space group $P2_1/c$; a = 9.655(2) Å, b = 11.210(2) Å, c = 19.798(4) Å, β = 91.36(3)°, V = 2142.2(7) Å^3, D_{calc} = 1.084 g cm^{-3}, Z = 4, F(000) = 764, λ = 0.71073 Å (graphite monochromated Mo Kα radiation), μ-(Mo Kα) = 0.253 mm^{-1}, T = 153 K. Data were collected with a Siemens Stoe AED on an oil-coated[58] rapidly cooled crystal of 0.3 × 0.3 × 0.6 mm^3 using the $2\theta/\omega$ scan method ($4° \le \theta \le 27.5°$). Of a total of 4960 collected reflections 4915 were unique and 3716 with $I > 2\sigma I$ observed. The structure was solved by direct methods using SHELXS-90;[59] 277 parameters were refined with all data by full matrix least squares on F^2 with a weighting scheme of $w^{-1} = \sigma^2(F_o)^2 + (0.057P)^2 + 0.90P$ with $P = (F_o + 2F_c^2)/3$ using SHELXL-92.[60] Final R-values: wR2 = 0.1391 (all data), and R1 = 0.049 (with $F > 4\sigma(F)$) (wR2 = $(\sum w(F_o^2 - F_c^2)^2/\sum w(F_o^2)^2)^{0.5}$; R1 = $\sum|F_o - F_c|/\sum F_o$). Largest peak and hole in the final difference map: 0.35 and –0.29 e Å^{-3}.

All non-hydrogen atoms were refined anisotropically. The benzylic hydrogen atoms (H(1) and H(2)) were refined using distance restraints for equivalent H-atoms. For all other hydrogen atoms a riding model was used.

Compound **1** crystallizes with one disordered toluene molecule on an inversion center. The latter was refined as one complete molecule with an occupation factor of 0.5 using distance restraints for equivalent 1,2 and 1,3 distances.

Crystal data for 2: (T = 200 ± 1 K; Siemens R3m/V diffractometer, crystals mounted in capillaries) M_r = 349.90, monoclinic, space group $C2/c$; a = 32.09(3) Å, b = 10.843(9) Å, c = 11.352(11) Å, β = 103.97-(8)°, V = 3834(6) Å^3, D_{calc} = 1.212 g cm^{-3}, Z = 8, F(000) = 1472, λ = 0.71073 Å (graphite monochromated Mo Kα radiation). Data were collected on a 0.3 × 0.3 × 0.4 mm^3 specimen using the ω-scan method ($3° \le 2\theta \le 54°$). Three standard reflections were measured every 100 reflections. From 6756 collected reflections 4218 were unique. The structure was solved by direct methods (SHELXTL PLUS 4.11). The complete data set was used for structure refinement by full matrix least squares on F^2 with a weighting scheme of $w^{-1} = \sigma^2(F_o)^2 + (0.2227P)^2 + 0.00P$, with $P = (F_o + 2F_c^2)/3$ using SHELXL-92;[60] 181 refined parameters. Final R-values: R1 = 0.1241 (for data with $F > 4\sigma(F)$); wR2 = 0.3082 (all data) (wR2 = $(\sum w(F_o^2 - F_c^2)^2/\sum w(F_o^2)^2)^{0.5}$ and R1 = $\sum|F_o - F_c|/\sum F_o$); largest peak (1.474 e Å^{-3}) and hole (–3.062 e Å^{-3}). All non-hydrogen atoms were refined anisotropically; the hydrogen atoms were fixed in idealized positions and refined using a riding model.

Further details of the crystal structure investigations are available on request from the Director of the Cambridge Crystallographic Data Centre, University Chemical Laboratory, 12 Union Road, GB-Cambridge CB2 1EZ, by quoting the full journal citation.

Computational Methods. Calculations were performed using the Gaussian 92 program package.[61] All geometries were fully optimized at the SCF and correlated level (MP2(full)) within the indicated symmetry constraints using standard gradient optimization techniques. For carbon,

(58) (a) Hope, H. *Experimental Organometallic Chemistry*; ACS Symposium Series 357; American Chemical Society, Washington, DC, 1987. (b) Hope, H. *Acta Crystallogr.* **1988**, *B44*, 22. (c) Kottke, T.; Stalke, D. *J. Appl. Crystallogr.* **1993**, *26*, 615.

(59) Sheldrick, G. M. *Acta Crystallogr.* **1990**, *A46*, 467.

(60) Sheldrick, G. M. SHELXL-92; University of Göttingen: Göttingen, Germany, 1992.

(61) Frisch, M. J.; Trucks, G. W.; Head-Gordon, M.; Gill, P. M. W.; Wong, M. W.; Foresman, J. B.; Johnson, B. G.; Schlegel, H. B.; Robb, M. A.; Replogle, E. S.; Gomperts, R.; Andres, J. L.; Raghavachari, K.; Binkley, J. S.; Gonzalez, C.; Martin, R. L.; Fox, D. J.; Defrees, D. J.; Baker, J.; Stewart, J. J. P.; Pople, J. A. *Gaussian 92*; Gaussian Inc.: Pittsburgh, PA, 1992.

hydrogen, lithium, and sodium, the 6-31G* basis set was used.[62] For the heavier alkali metals (K–Cs), we employed the Huzinaga minimal basis sets,[63] with the highest s and p shells split and additional diffuse p and d functions. The contraction schemes were K, 43321/4211/1, p = 0.039, d = 0.794; Rb, 433321/43211/41, p = 0.034, d = 0.541; Cs, 4322211/42221/421, p = 0.026, d = 0.353. Stationary points were characterized as minima or transition structures by calculating the vibrational frequencies at the SCF level. Natural charges were calculated by using the natural population analysis (NPA) method.[51]

Calculations of the periodic polymers were performed employing the ab initio Hartree–Fock crystal orbital method[64,65] in the first neighbors' approximation. The details of this formalism have been discussed elsewhere.[54,66,67] A minimal Clementi basis set[68] was used for all atoms.

Acknowledgment. This work was supported by the Fonds der Chemischen Industrie and the Deutsche Forschungsgemeinschaft. We greatly acknowledge the earlier contributions of Dr. R. Hacker and Dr. C. Schade to the transmetalation procedures used in this work. We are indebted to Chemetall GmbH (Franfurt a. Main) for the generous gift of rubidium metal and to the Riedel de Haën AG (Seelze) for supplying the polyfluoropolyethers applied in crystal mounting.

Supplementary Material Available: Tables of bond distances, bond angles, atomic coordinates, anisotropic displacement parameters, and ORTEP plots (17 pages) for **1** and **2**; tables of observed and calculated structure factors for **1** and **2** (20 pages). This material is contained in many libraries on microfiche, immediately follows this article in the microfilm version of the journal, and can be ordered from the ACS; see any current masthead page for ordering information. Optimized geometries are available as "archive entries" from the authors on request.

(62) (a) Hariharan, P. C.; Pople, J. A. *Theor. Chim. Acta* **1973**, *28*, 213. (b) Dill, J. D.; Pople, J. A. *J. Chem. Phys.* **1975**, *62*, 2921. (c) Francl, M. M.; Pietro, W. J.; Hehre, W. J.; Binkley, J. S.; Gordon, M. S.; Defrees, D. J.; Pople, J. A. *J. Chem. Phys.* **1988**, *77*, 3654.

(63) Huzinaga, S. *Gaussian basis sets for molecular calculations*, physical sciences data 16; Elsevier: Amsterdam, 1984.

(64) André, J. M.; Gouverneur, L.; Leroy, G. *Int. J. Quantum. Chem.* **1967**, *1*, 427, 451.

(65) Del Re, G.; Ladik, J.; Biczó, G. *Phys. Rev.* **1967**, *155*, 997.

(66) Ladik, J. In *Electronic Structure of Polymers and Molecular Crystals*; André, J. M., Ladik, J., Delhalle, J., Eds.; Plenum Press: New York, 1975; p 633.

(67) Ladik, J. In *Quantum Theory of Polymers as Solids*; Plenum Press: New York, 1988.

(68) Gianolio, L.; Pavani, R.; Clementi, E. *Gazz. Chim. Ital.* **1978** *108*, 181.